






Centrifugal model tests and numerical simulations for barrier dam break due to overtopping

ZHAO Tian-long^{1,2}  <https://orcid.org/0000-0002-1912-1502>; e-mail: Neo_3303@163.com

CHEN Sheng-shui²  <https://orcid.org/0000-0002-9613-0488>; e-mail: sschen@nhri.cn

FU Chang-jing^{1*}  <https://orcid.org/0000-0001-7398-5603>;  e-mail: 546684412@qq.com

ZHONG Qi-ming³  <https://orcid.org/0000-0001-6077-5252>; e-mail: qmzhong@nhri.cn

* Corresponding Author

¹ Key Laboratory for Hydraulic and Waterway Engineering of Ministry of Education, Chongqing Jiaotong University, Chongqing 400074, China

² Nanjing Hydraulic Research Institute, Key Laboratory of Failure Mechanism and Safety Control Techniques of Earth-rock Dam of the Ministry of Water Resources, Nanjing 210029, China

³ Department of Geotechnical Engineering, Nanjing Hydraulic Research Institute, Nanjing 210029, China

Citation: Zhao TL, Chen SS, Fu CJ, et al. (2019) Centrifugal model tests and numerical simulations for barrier dam break due to overtopping. *Journal of Mountain Science* 16(3). <https://doi.org/10.1007/s11629-018-5024-0>

© Science Press, Institute of Mountain Hazards and Environment, CAS and Springer-Verlag GmbH Germany, part of Springer Nature 2019

Abstract: The present study focuses on the breaching process and failure of barrier dams due to overtopping. In this work, a series of centrifugal model tests is presented to examine the failure mechanisms of landslide dams. Based on the experimental results, failure process and mechanism of barrier dam due to overtopping are analyzed and further verified by simulating the experimental overtopping failure process. The results indicate that the barrier dam will develop during the entire process of overtopping in the width direction, whereas the breach will cease to develop at an early stage in the depth direction because of the large particles that accumulate on the downstream slope. Moreover, headcut erosion can be clearly observed in the first two stages of overtopping, and coarsening on the downstream slope occurs in the last stage of overtopping. Thus, the bottom part of the barrier dam can survive after dam breaching and full dam failure becomes relatively rare for a barrier dam. Furthermore, the remaining breach would be smaller

than that of a homogeneous cohesive dam under the same conditions.

Keywords: Barrier dam; Overtopping; Failure mechanism; Centrifugal model test; Numerical simulation

Introduction

Landslide dams, presented as a natural blockage of a river by the hill slope-derived mass movement, are rather common in hilly and mountainous areas (Cao et al. 2011). Typical examples include the October 1999 case in the Poerua River in Westland, South Island, New Zealand (Davies et al. 2007) and the June 1967 case in the Yalong River in China (Li et al. 1986; Chen et al. 1992). Most recently, on May 12, 2008, a major earthquake occurred in Sichuan Province in China, which led to the formation of more than 100 landslide dams (e.g., Hu et al. 2009; Cui et al.

Received: 15-May-2018

Revised: 11-Nov-2018

Accepted: 21-Jan-2019

2009). Due to its random formation process, the material composition and structural characteristics of barrier dams are very different from those of the man-made earth-rock dams. Because of these differences, landslide dams are extremely prone to breaking owing to a variety of processes including overtopping, instability of the dam slope, or piping and most of them eventually disintegrate in a year (Kuang 1993; Yan et al. 2009; Schuster et al. 1986; Mizuyama et al. 2008; Wan et al. 2004). Barrier dams usually break in a short time after they are formed (Peng et al. 2012). Their life expectancy statistics are presented in Figure 1. Once a dam breaks down, it can easily cause severe flooding. Thus, a better understanding of the dam breach development is required to take adequate engineering measures to prevent further damage.

Since it is difficult to measure real-time water levels during flood events, experiments are carried out in laboratories to enhance the understanding of breaching hydraulics. In the past several decades, physical model tests have played an important role in the study of dam failure mechanisms (Li et al. 2009; Zhao et al. 2017; Tacconi et al. 2016). Experimental research on an artificial-dam break can be traced back to the middle of the 19th century. Numerous experimental studies on the breaching process and the failure mechanism of artificial clay dams (homogeneous earth dams and core dams) due to overtopping or piping have been conducted; e.g., the National Dam Safety Program (NDSP) by the US Federal Emergency Management Agency (FEMA; Corns 2010); the CADAM Project, a concerted-action project funded under the European Commission (EC) FP4 Program (Morris 2000); the 2001 IMPACT project; and the 2004 FLOODsite Project, another EC-funded integrated project (Morris et al. 2005; Bruijn et al. 2009). In recent years, a series of barrier-dam failure model tests based on the artificial-dam erosion models have been performed (Davies et al. 2007; Jiang 2007; Wang et al. 2008; Gregoretti et al. 2010; Davies 2002; Zhao et al. 2017). Experimental research on breach growth processes in the landslide dams of the quake lakes was carried out by Yang et al. (2011) and the angle of repose for uniform sediment particles was studied. Cao et al. (2011) presented a series of experiments in a flume to study landslide dam failure and flooding. Xuan et al. (2016) conducted a

series of experiments describing the landslide dam failure due to overtopping in three dimensions (3D) and proposed a two-dimensional (2D) surface flow erosion model to simulate the breach.

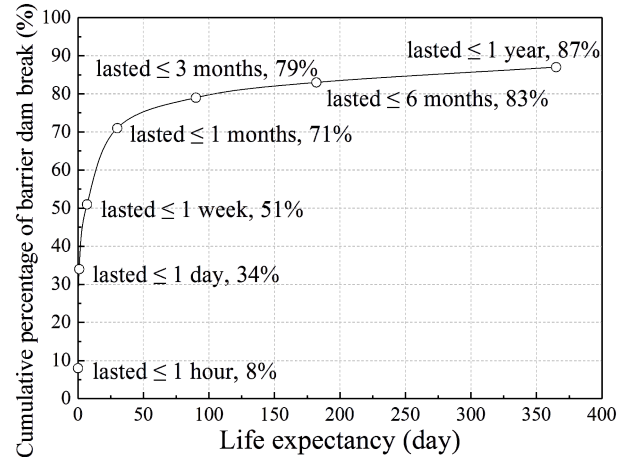


Figure 1 Age of landslide dams at time of failure (Peng et al. 2012).

To the best of our knowledge, most of the dam-break experimental research has focused on explaining the breaching mechanism of man-made earth-rock dams and most of the previous physical experiments are constrained by the comparatively small spatial scales. Only a few real landslide breaching data that exist are predominantly from the interviews and non-quantitative observations by witnesses (Becker et al. 2007; Zhong et al. 2018). The understanding of the mechanism of landslide dam failure and floods has so far remained poor and observational data sparse, which constitutes one of the basic impediments to the calibration and testing of the mathematical models (Cao et al. 2011).

This study aims to investigate the barrier-dam failure due to overtopping through centrifugal experiments and numerical simulations. Based on the similarity scales, the centrifugal model test of barrier dam overtopping has recently been performed and the experimental overtopping process has been simulated using a numerical model. In this study, the processes and mechanisms of barrier dam overtopping are addressed and the rules of breach development in horizontal and vertical directions, as well as the headcut erosion mechanism on a downstream slope, are revealed.

1 Experimental Apparatus and Methods

1.1 Experimental apparatus

Model tests of barrier dam overtopping are conducted based on the centrifugal model test system of the Nanjing Hydraulic Research Institute (NHRI). The dam-break test system consists of a geotechnical centrifuge, an automatic flow control system, a special model box, and a data and image acquisition system. The main equipment of the system is a 400 gt geotechnical centrifuge (Figure 2a). The maximum acceleration of the centrifuge is 200 g and the maximum payload is 2 t.

The task of the automatic water flow control system is to provide sufficient and stable water supply during the dam-break test. The water flow control system includes a water tank, a pipeline, a

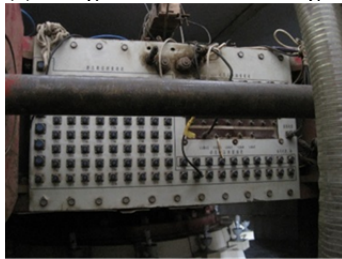
flowmeter, and a water-ring (Figure 2b). This system can be used to precisely control the water supply in the test (Chen et al. 2018).

Model box is an essential device in this test system. The internal effective size of the model box is 1.2 m×0.4 m×0.8 m. One side of the box is comprised of PMMA (polymethyl methacrylate) to observe the dam-break process during the experiment (Figure 2c). The downstream side of the model box is designed with a rectangular sharp-crested weir, which is used to monitor water flow (Lobovsky et al. 2013; Zhao et al. 2018).

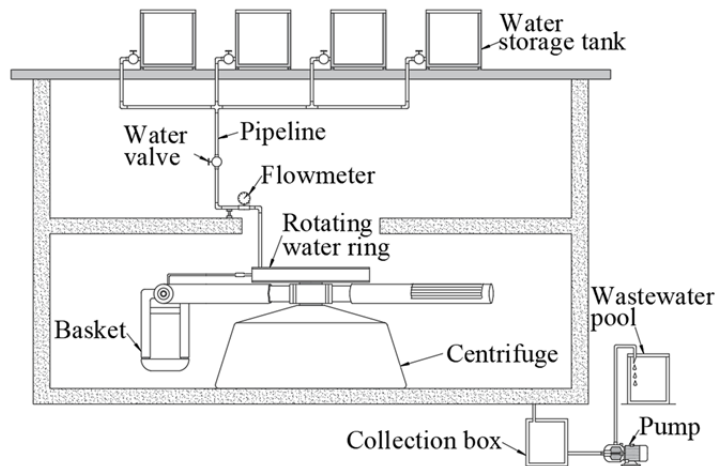
Data acquisition of the centrifugal model test system is composed of an isolated measurement pod (IMP) data acquisition module and an industrial personal computer (IPC). As shown in Figure 2d. In addition, through cameras placed on the model box, the failure process of the barrier



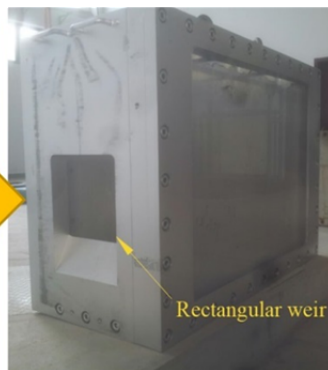
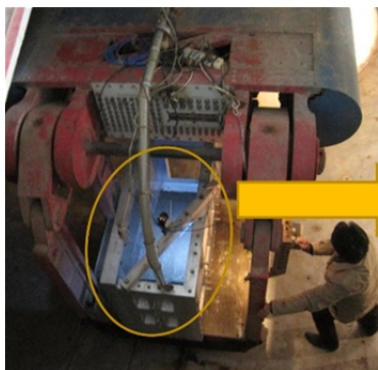
(a) The geotechnical centrifuge



(d) Data acquisition module



(b) Water supply system



(c) The basket of the centrifuge and the model box

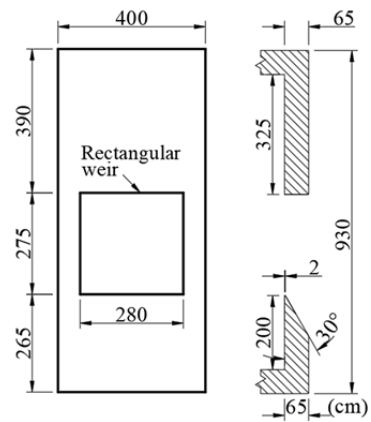


Figure 2 Centrifugal model test system.

dam can be monitored.

1.2 Model design

1.2.1 Preparation of model dam material

Wide gradation of dam materials is a remarkable feature of barrier dams. In this experiment, material gradation of the Tangjiashan landslide dam is considered. In the centrifugal model box, the maximum particle size of the test material is controlled at 20 mm. Because there is no definite functional relationship for clay between the critical shear stress and the average particle size (Chen et al. 2011; Butterfield 1999), the clay content is consistent with the Tangjiashan landslide dam material, whose value is 13% (Liu et al. 2010). According to the grading curve of the Tangjiashan landslide dam, an equivalent substitution method is adopted to replace the particles with sizes larger than 20 mm with those with sizes of 0.075–20 mm. The gradation curve of the model dam material is shown in Figure 3.

In addition, $\rho_m = \rho_p$ (ρ_m , density of prototype materials; ρ_p , density of model materials) in the centrifugal model tests; therefore, it is necessary to ensure that the model dam has the same dry density as the Tangjiashan landslide dam, whose value is 1.59 g/cm³. The basic parameters of the model dam material are shown in Table 1.

In particular, this experiment did not fully simulate the discharge process of the Tangjiashan barrier dam. The similarity of the granular materials of the landside dam is just to make sure that the material of the model dam is wide-graded.

1.2.2 Construction of model dam

The angle of the dam downstream slope has an important influence on the development of a breach and the break flow. Thus, in the design of the model dam, the slope angle of the barrier dam should be adequately small. According to the internal dimensions of the model box, the slope ratio of the dam downstream is 1:3.5, the dam crest width is 20 cm, the dam height is 20 cm, and the upstream slope ratio is 2:1. On the downstream of the model dam, the tail water, which is 5 cm in depth, is used for the weir flow calculation.

To study the breach development process, an inverted trapezoid groove (Figure 4a) is excavated

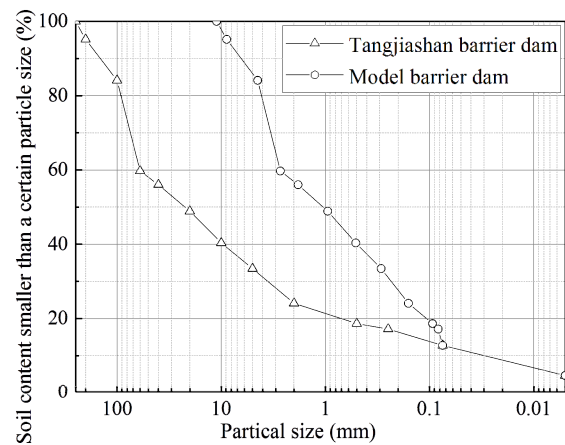


Figure 3 Gradation curves of model dam and the gradation of Tangjiashan barrier dam.

Table 1 Parameters of model dam material

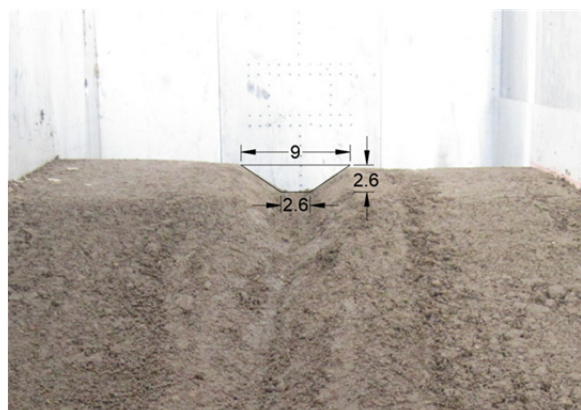
Index	Median diameter (d_{50} , mm)	Restricted particle Diameter (d_{60} , mm)	
Value	1.1	2.7	
Index	Dry density (ρ_d , g/cm ³)	Porosity (n , %)	Permeability coefficient (k , cm/s)
Value	1.59	0.4	1.0×10^{-3}

from the middle of the dam crest as an initial breach to avoid the break water flow across the whole dam crest. The size of the groove is 9.0 cm in the top width, 2.6 cm in the bottom width, and 2.6 cm in depth.

The model dam is constructed with a dry density of 1.59 g/cm³. The outlet of the water supply pipeline is located at the bottom of the upstream slope. To prevent water supply from directly eroding the upstream slope, the outlet is wrapped with gauze. The internal overall layout of the model box is shown in Figure 4b and 4c.

2 Experimental Procedure and Data

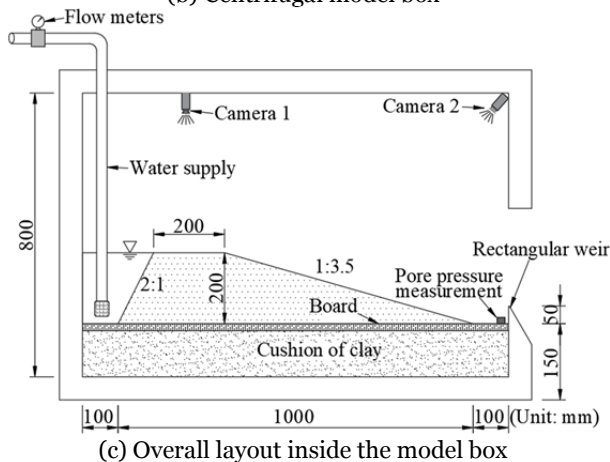
In the centrifugal model tests of barrier dam overtopping, the centrifugal acceleration was set to 30 g and the water supply flow in the tests was set to 0.02 m³/s. It means that the model tests simulated the overtopping process of barrier dams in 6 m height, and the self-weight stress inside the model dam is consistent with that of the prototype dam with a height of 6 m. During the test, the model dam was continued to be observed until no deformation appeared at the breach and the downstream slope under this flow condition. Then, water supply was stopped accordingly.



(a) Initial breach of model dam (Unit: cm)



(b) Centrifugal model box



(c) Overall layout inside the model box

Figure 4 Overall layout of the centrifugal model box and the model dam.

2.1 Process of dam failure

Two sets of centrifugal model tests of barrier dam overtopping were conducted and the results showed a consistent failure process (Figure 5). Based on Figure 5, barrier dam failure by overtopping can be obtained as follows.

(1) Figure 5a shows that the initial notching forms on the downstream slope 6.5 min after dam

break. Notch cutting is fast at this stage and headcut forms gradually. Headcut erosion and small scarps in notching can be observed on the downstream slope.

(2) Twenty minutes after the dam break (Figure 5b), headcut formed in the previous stage begins to move towards the dam crest and source-tracing erosion is observed. At this stage, breach flow mainly erodes the side slope of the breach, resulting in the fast expansion of the breach width.

(3) After 35 min, it is difficult to maintain the steepness for the breach-side slope under continuous erosion and the dam begins to collapse (Figure 5c). Hence, the breach width alternately expands in the form of continual erosion and collapses on the side slopes. Owing to the new expansion form, the breach width expansion is much faster than that of the previous stage.

(4) Sixty minutes after the dam break, breach width expansion and vertical cutting slows down gradually. Small particles are nearly washed away and large particles, such as gravel and boulders, remain on the downstream slope, resulting in the coarsening of the downstream slope (Figure 5d). Owing to the existence of large particles on the dam slope, further breach development is prevented under a certain hydraulic condition.

2.2 Residual dam

2.2.1 Dam crest and upstream slope

Figure 6a shows the crest and the upstream slope of the residual dam. Under centrifugal acceleration and reservoir water infiltration, there is a certain amount of settlement in the dam body (Figure 6a). The model dam is constructed and consolidated under the gravity of 1 g; however, under the gravity of 30 g during the centrifugal model tests, the model dam is under-consolidated. Therefore, under the effect of space-time compression of the centrifugal test and reservoir water infiltration, consolidation of the model dam material is completed in a short time and the final settlement is 0.72 m.

For upstream dam slopes, the shear strength of dam materials decreases due to reservoir water infiltration and the original slope can no longer be maintained. Thus, Figure 6a shows the collapse of the upstream slope of the model dam and there is siltation of dam materials after collapse on the

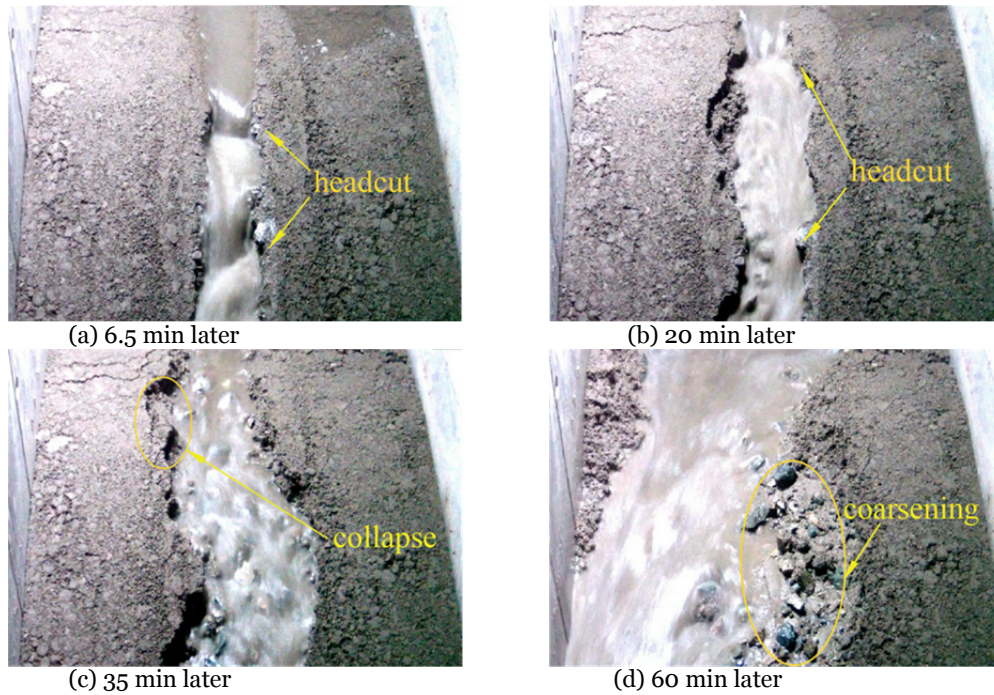


Figure 5 Breaching process due to overtopping.

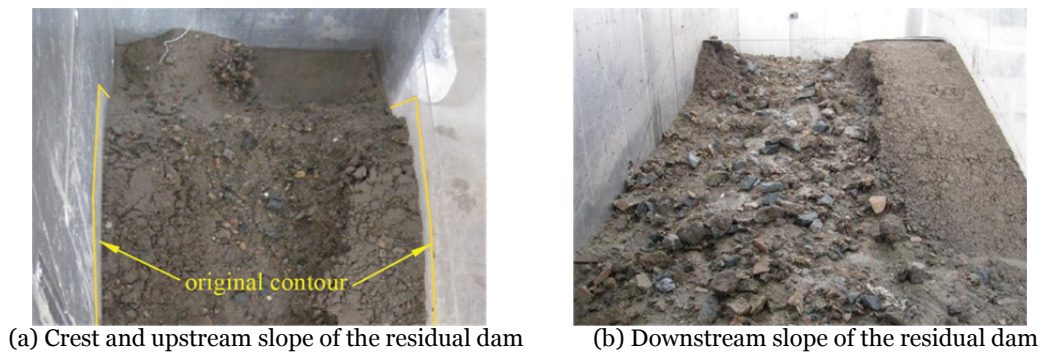


Figure 6 Residual dam after overtopping.

right side of upstream.

2.2.2 Downstream slope

Figure 6b shows the downstream slope of the residual dam. The right side of the downstream dam slope is more severely eroded and breach remaining is located on the right side of the dam crest. The top and bottom width of breach remaining is 6.3 m and 5.5 m, respectively. Gravels that remain on the downstream slope after the experiments prevent the breach from further scouring and vertical cutting. The breach bottom elevation of the residual dam is 4.4 m.

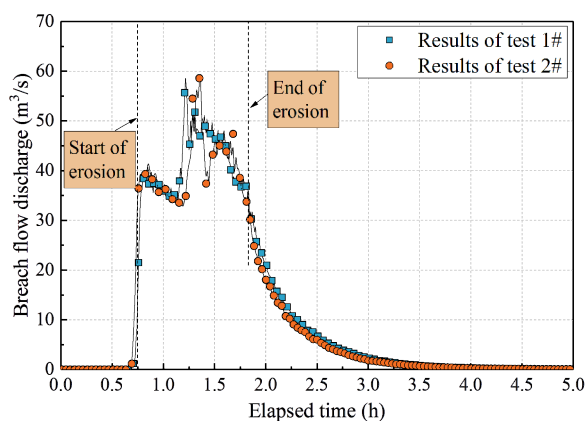
2.3 Discharge process analysis

The curve of the breach flow was calculated

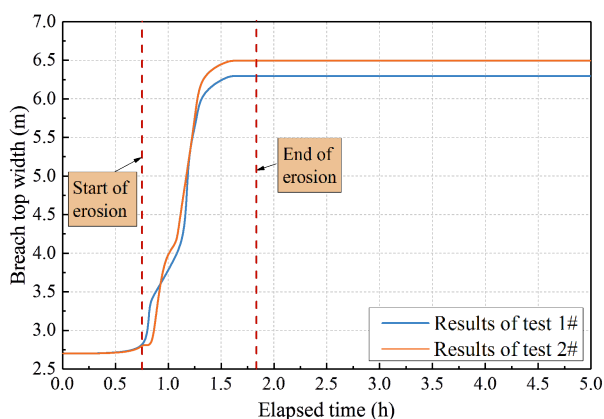
using the monitoring data from the rectangular weir. In this experiment, the downstream water level was low. Because of the shielding of the upper part of the model box, the wind field in the centrifuge room (while running) had minimal influence on the entire testing process. The weir water head in the prototype scale could be acquired by centrifugal acceleration, following the specification for the rectangular weir flow calculation. Using the data of the two sets of the barrier-dam break centrifugal model tests, breach flow curves were calculated (Figure 7a). In Figure 7a, the elapsed time starts when the model dam upstream begins to store water. The elapsed time and breach flow are analyzed in the prototype scale according to centrifugal acceleration. The elapsed

time is the inertial time, whose scale relation is $1/N$.

Figure 7a shows that breach flow of the two sets of tests is low during a relatively long time period at the beginning of the dam break; the value is approximately $1.5 \text{ m}^3/\text{s}$. Approximately 0.68 h after the dam failure, discharge of the breach flow sharply increases with an acceleration rate of $0.161 \text{ m}^3/\text{s}^2$ and the breach flow in the first set of tests is approximately 0.02 h later than that of the second set. Through the previously analyzed failure mechanism, breach development is dominated by notch cutting at this stage. Thus, when the dam erosion begins, the breach bottom elevation rapidly decreases and the water head increases sharply with the increase in breach flow.



(a) Breach flow hydrograph for experimental tests



(b) The development of breach top width

Figure 7 Breaching parameters of landslide dams.

Approximately 0.85 h later, breach flow in two sets of experiments reached $40.6 \text{ m}^3/\text{s}$ and decreased at the same rate because the breach bottom cutting to the final elevation was under the effect of the flow discharge. Then, the water head

gradually decreased, causing a decrease in the flow rate following the peak flow. Thereafter, the breach flow increased again to $60.2 \text{ m}^3/\text{s}$ and the flood peak time of the two sets of tests was 1.21 h and 1.25 h , respectively. At this stage, breach flow had the strongest erosion capability and breach development was dominated by width expansion. Since the breach soil on both sides was washed away, breach width continually expanded and breach flow fluctuated during this time. Subsequently, breach flow decreased and the scour process gradually disappeared. The breach was fully developed at this point. Meanwhile, the armor layer appeared on the downstream slope and the entire dam-break process concluded.

2.4 Analysis of breach top width development process

The breach top width development process was documented by a dam-break video. The elapsed time was calculated by the scale relation of inertial time, whose value was $1/N$. The breach top width development is shown in Figure 7b. In this figure, the development process corresponds to the breach flow discharge process. At the beginning, the pace of the breach horizontal expansion was slow. Meanwhile, the development speed of the breach top width increased significantly at approximately 0.68 h after overtopping and the value was approximately 10.5 m/h . At this stage, breach flow also sharply increased.

Approximately 0.85 h later, the expansion of the breach top width began to slow down and breach flow decreased with a decrease in dam erosion. Approximately 1.17 h later, breach flow increased once again and the breach width expansion sped up accordingly. Approximately 1.49 h later, the breach top width expansion gradually slowed and marked the cessation of dam erosion. The remaining breach top widths were 6.30 m and 6.50 m , respectively, through the two sets of model tests. These results indicated that the development of the breach width extended through the entire dam-break process. In the early stages, breach width expansion was slower than the notch cutting. As the breach flow decreased, the breach was cut into the final elevation of the bottom in a very short time period. From that point, breach development was dominated by width expansion.

3 Numerical Simulation and Analysis

The centrifugal model test process is complex; it is difficult to test the dam break under different conditions (Wang et al. 2017). Therefore, the NWS BREACH model is adopted to simulate the experimental breaching process and further analyze the breach process under different conditions for comprehensively evaluating the barrier dam failure mechanism due to overtopping.

3.1 NWS BREACH model

The US National Weather Service (NWS) BREACH model was proposed by Fread (1988). The model calculates the failure process of earth-rock dams caused by overtopping and piping. The model assumes that there is an initial (generalized) breach with a rectangular cross-section at the dam crest and the downstream slope. During the failure process, the breach is parallel to the dam crest and the downstream slope. The model also assumes that the erosion rate of the breach bottom is equal to that of the both sides of the breach. The simplified overtopping failure process based on the NWS BREACH model assumptions is shown in Figure 8.

In this model, the change in the reservoir water level is calculated using the water balance equation.

$$A_s \frac{dz_s}{dt} = Q_{in} - Q - Q_{spill} - Q_{sluice}, \quad (1)$$

where A_s = surface area of the reservoir, z_s = water surface elevation, t = time, Q_{in} = inflow discharge, Q = breach flow, Q_{spill} = flow through spillways, and Q_{sluice} = flow through sluice gates. The breach flow is calculated using the wide crest weir equation.

$$Q = k_{sm} (c_1 b h^{1.5} + c_2 m h^{2.5}), \quad (2)$$

where b = bottom width of breach, h = height difference between the reservoir water level and the breach bottom, m = breach side slope coefficient, $c_1 = 1.7$, $c_2 = 1.3$ (Wu 2013), k_{sm} = submerging coefficient and the parameter k_{sm} is not considered in this calculation.

The width of the initial breach can be calculated using Eq. (3).

$$b_0 = B_r y, \quad (3)$$

where $B_r = 2$ (Zhong et al. 2016) and y = water depth at initial breach (Eq. 4).

$$y = \frac{2}{3} (z_s - z_b), \quad (4)$$

where z_b = elevation of breach bottom. The modified Meyer-Peter and Mueller formulas are used for estimating the material transport in the dam break.

$$Q_s = 3.64 \left(\frac{d_{90}}{d_{30}} \right)^{0.2} P \frac{h^{2/3}}{n} S^{1.1} (hS - \Omega), \quad (5)$$

where Q_s = erosion rate of dam materials, d_{90} = particle size with 90% content, d_{30} = particle size with 30% content, P = wetted perimeter, n = Manning coefficient, S = breach side slope ratio, Ω = threshold related to dam material properties. Manning coefficient can be calculated using Eq. (6).

$$n = d_{50}^{0.167} / A_n, \quad (6)$$

where $A_n = 76.9$ (Liu et al. 2016). The stability of the breach side slope is closely related to the cut depth. The breach side slope will collapse if it exceeds the critical depth. In this model, the critical cut depth of the breach is calculated using Eq. (7).

$$h_c = \frac{4c \cos \varphi \sin \theta}{\gamma [1 - \cos(\theta - \varphi)]}, \quad (7)$$

where h_c = critical cut depth of breach, c = cohesion of dam material, φ = internal friction angle of dam material, θ = breach side slope angle,

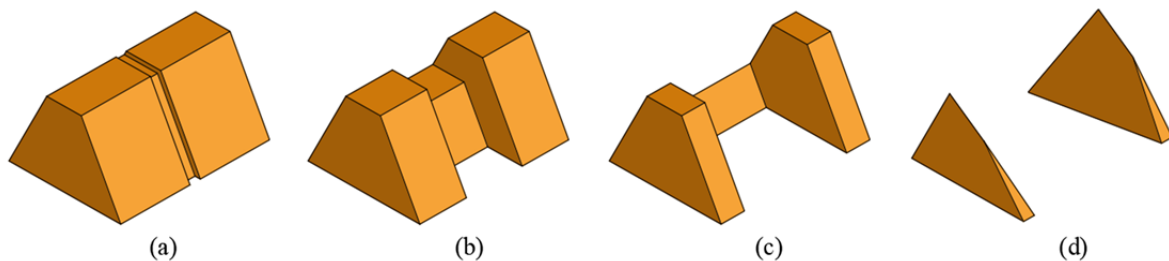


Figure 8 Simplified overtopping failure process based on NWS BREACH model assumptions.

and γ = dam material unit weight. The calculation method of this model is the time-based iteration. The procedure of the dam breach due to overtopping is presented in Figure 9.

3.2 Experimental procedure simulation

The NWS BREACH model is adopted to simulate the experimental barrier dam failure procedure due to overtopping. Values of the parameters used in the simulation are listed in Table 2.

3.2.1 Verification of the selected parameters

Breach flow is a very important parameter in the mechanism and process analysis of dam break. Figure 10 compares the measured and calculated breach flow values. Results of the numerical simulation are close to those of the experiments. Approximately 0.68 h after the dam failure, breach flow sharply increases. The peak flow and time measured in the tests are 56.6 m³/s and 1.23 h, respectively, and the calculated ones are 55.0 m³/s and 1.25 h, respectively. After the peak flood, breach flow decreases gradually and the calculated reduction rate coincides with the measured one.

Therefore, it is appropriate to select the NWS BREACH model for the numerical simulation of the barrier dam overtopping process and the parameters selected in the model calculation step are reasonable.

3.2.2 Development of breach and reservoir water

Due to the turbidity of the overflow, it is difficult to accurately measure the reservoir water level and the height and width of the breach bottom during the tests. Therefore, the NWS breach model is adopted to simulate the experimental overtopping process, from which the parameters such as the reservoir water level and the breach bottom elevation and width can be easily extracted. The model results are shown in Figure 11. In Figure 11, with the outbreak of dam failure, the reservoir water level keeps rising and notch cutting of breach develops rapidly. However, lateral expansion of the breach is relatively slow at this stage. After 0.65 h, notch cutting of the breach begins to increase sharply and it has a value of 3.47 m/s. At this stage, the water head is 0.55 m, the

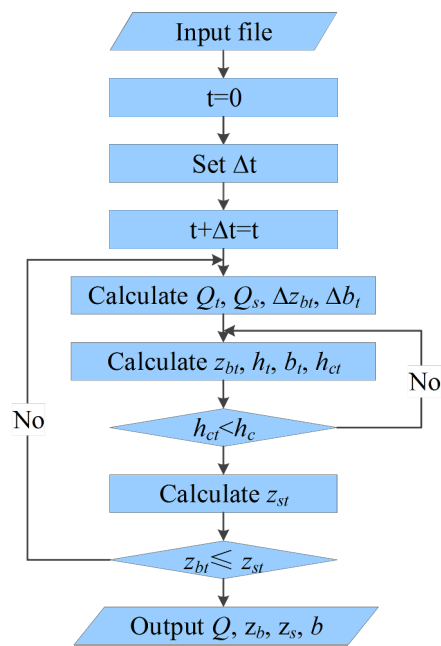


Figure 9 Algorithm of the NWS BREACH model.

Table 2 Values of the parameters used in the simulation

Index	ρ (kg/m ³)	μ (Pa·s)	h_d (m)	l_d (m)	m_d (V/H)	b_o (m)	z_{bo} (m)
Value	1000	0.001	6	12	0.286	0.78	5.22
Index	n	d_{50} (m)	G_s	Φ	c (Pa)	φ	z_{so} (m)
Value	0.045	0.051	2.65	0.4	25000	22.0	5.25

Note: ρ = fluid density, μ = dynamic viscosity, h_d = dam height, l_d = dam length, m_d = slope coefficient of downstream, V/H = vertical length/horizontal length, b_o = initial breach width, z_{bo} = initial breach bottom height, n = Manning coefficient, d_{50} = median size of soil, G_s = specific gravity of soil, Φ = porosity, c = soil cohesion, φ = friction angle, and z_{so} = initial reservoir level.

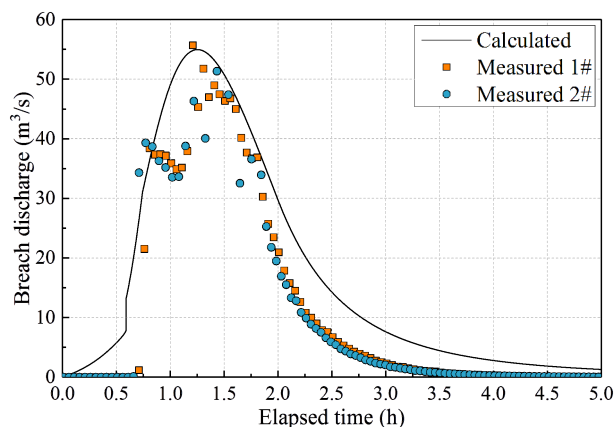


Figure 10 Comparison of measured and calculated breach flow hydrographs and top width.

width of the breach begins to increase continuously, and intermittent collapses begin to appear on the

breach-side slopes. Then, the width of the breach continues to increase, but the development of notch cutting gradually stagnates. With the decrease of the water head, lateral expansion of the breach stops.

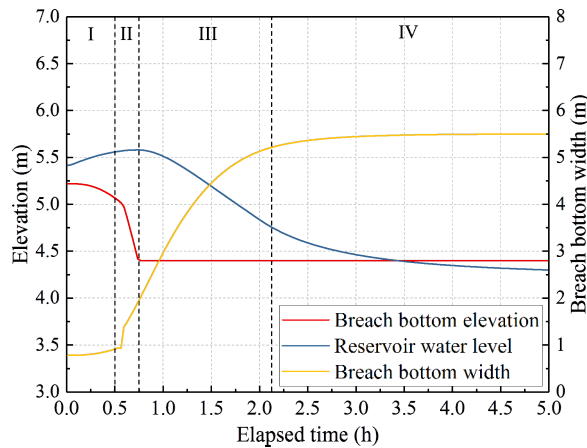


Figure 11 Development of breach and reservoir water.

The mechanism of barrier dam overtopping failure revealed by the numerical simulation agrees with the experimental results. Longitudinal development of the breach starts earlier than the lateral expansion but lasts for a short time. In the latter stage of the dam break, lateral expansion is the main form of breach development. Because the vertical development of breach stops at an early time, the residual barrier dam will survive after the dam break.

4 Concluding Remarks

In this study, centrifugal model tests of dam failure due to overtopping were conducted and experimental overtopping process was simulated using a numerical model. The results can be summarized as follows:

(1) A dam-break centrifugal model test system is established and a series of experiments on barrier dam overtopping are performed. The applicability of the centrifugal model test in dam-break research is verified.

(2) The barrier dam overtopping process is divided into four stages, i) headcut forms gradually and notch cutting of breach develops fast, ii) vertical development slows down after source-tracing erosion and the breach develops rapidly in the width direction, iii) the breach-side slope

begins to collapse, iv) breach development gradually stops and coarsening of the downstream slope is observed.

(3) In the latter period of the barrier dam break, the armor layer appears on the downstream slope. Large particles accumulate on the downstream slope and prevent further development of the breach. Therefore, in practice, the bottom part of the barrier dam, which consists of earth and stone material with wide grading, would survive after dam breaching. The complete dam failure is quite rare for a barrier dam.

(4) In these four stages, breach development in width and depth directions have no simultaneity. Breach depth development mainly occurs in the first two stages. Due to the coarsening of the downstream slope, vertical development of the breach stops at an early time. Development of the breach width extends through the entire dam-break process and becomes faster in the second and third stages.

(5) Previous studies predicted the behavior of barrier dam downstream erosion is mainly surface scouring, and headcut erosion is rarely observed in the overtopping process for barrier dam. However, the occurrence of headcut erosion is related to the clay content of dam materials. In this tests, headcut erosion can be obviously observed under the clay content of %. Therefore, whether the headcut and source-tracing erosion occurs or not during the breaching is closely related to the barrier dam material source condition.

(6) The size of the remaining breach is less than that of the homogeneous earth dam under the same conditions. During the risk assessment and prediction of flooding caused by the barrier dam break, compared to the entire dam-break, the condition of the partial dam break must be fully considered.

Acknowledgments

The authors gratefully acknowledge the financial support from the National Natural Science Foundation of China (Grant No. 51709025), the Chongqing Science and Technology Commission of China (Grant No. cstc2018jcyjAX0084, cstc2018jcyjAX0391 and cstc2016jcyjA0551), Open Research Fund of Key

Laboratory of Failure Mechanism and Safety Control Techniques of Earth-Rock Dam of the

Ministry of Water Resources (Grant No. YK319006), respectively.

References

- Andrea M, Marco P, Massimo T (2017) Experimental and Numerical Analysis of Side Weir Flows in a Converging Channel. *Journal of Hydraulic Engineering* 143 (7). [https://doi.org/10.1061/\(ASCE\)HY.1943-7900.0001296](https://doi.org/10.1061/(ASCE)HY.1943-7900.0001296)
- Becker JS, Johnson DM, Paton D (2007) Response to landslide dam failure emergencies: Issues resulting from the October 1999 Mount Adams landslide and dam-break flood in the Poerua River, Westland, New Zealand. *Natural Hazards Review* 2(8): 35-42. [https://doi.org/10.1061/\(ASCE\)1527-6988\(2007\)8:2\(35\)](https://doi.org/10.1061/(ASCE)1527-6988(2007)8:2(35))
- Bruijn KD, Klijn F, Ölfert A, et al. (2009) Flood risk assessment and flood risk management. An introduction and guidance based on experiences and findings of FLOOD site (an EU-funded Integrated Project). *Deltares*.
- Cao Z, Yue Z, Pender G (2011) Landslide dam failure and flood hydraulics. Part I: experimental investigation. *Natural Hazards* 59 (2): 1003-1019. <https://doi.org/10.1007/s11069-011-9814-8>.
- Chen S, Xu G, Zhong Q, Gu X (2012) Development and application of centrifugal model test system for break of earth-rock dams. *Journal of Hydraulic Engineering* 43 (2): 241-245. (In Chinese) <https://doi.org/10.13243/j.cnki.slxb.2012.02.006>
- Chen Y, Zhou F, Feng Y, et al. (1992) Breach of a naturally embanked dam on Yalong River. *Canadian Journal of Civil Engineering* 19 (5): 811-818. <https://doi.org/10.1139/l92-092>
- Corns CF (2010) Status Report on the National Dam Safety Program. Paper read at Safety of Small Dams. pp 4-7.
- Cui P, Zhu Y, Han Y, et al. (2009) The 12 May Wenchuan earthquake-induced landslide lakes: distribution and preliminary risk evaluation. *Landslides* 6 (3): 209-223. <https://doi.org/10.1007/s10346-009-0160-9>
- Davies TR (2002) Landslide-dambreak floods at Franz Josef Glacier township, Westland, New Zealand: a risk assessment. *Journal of Hydrology (New Zealand)* 41 (1):1-17.
- Davies TR, Manville V, Kunz M, et al. (2007) Modeling landslide dambreak flood magnitudes: Case study. *Journal of Hydraulic Engineering* 133 (7):713-720. [https://doi.org/10.1061/\(ASCE\)0733-9429\(2007\)133:7\(713\)](https://doi.org/10.1061/(ASCE)0733-9429(2007)133:7(713))
- Fread DL (1988) BREACH: An erosion model for earthen dam failure. US National Weather Service Report, Silver Spring.
- Gregoretti C, Maltauro A, Lanzoni S (2010) Laboratory experiments on the failure of coarse homogeneous sediment natural dams on a sloping bed. *Journal of Hydraulic Engineering* 136 (11): 868-879. [https://doi.org/10.1061/\(ASCE\)HY.1943-7900.0000259](https://doi.org/10.1061/(ASCE)HY.1943-7900.0000259)
- Hu X, Lu X, Huang R, et al. (2009) Developmental features and evaluation of blocking dangers of Dashui ditch debris flow in Tangjiashan dammed lake. *Chinese Journal of Rock Mechanics & Engineering* 28 (4): 850-858. (In Chinese) <https://doi.org/10.3321/j.issn:1000-6915.2009.04.026>
- Jiang H (2007) Study on process of barrier dam break and the flow change. *Technology of Soil and Water Conservation* (1): 24-26. (In Chinese) <https://doi.org/10.3969/j.issn.1673-5366.2007.01.009>
- Kuang S (1993) Formation Mechanisms and Prediction Models of Debris Flow due to Natural Dam Failures. *Journal of Sediment Research* (4): 42-57. (In Chinese) <https://doi.org/10.16239/j.cnki.0468-155x.1993.04.006>
- Li T, Schuster R, Wu J (1986) Landslide dams in south central China. *Landslide Dams Processes Risk & Mitigation*. Schuster RL (ed.). American Society of Civil Engineers, Geotechnical Special Publication, 3: 146-162.
- Li Y, Li J (2009) Review on experimental study on dam-break. *Advances in Water Science* 20 (2): 304-310. (In Chinese) <https://doi.org/10.3321/j.issn:1001-6791.2009.02.024>
- Liu N, Chen Z, Zhang J, et al. (2010) Draining the Tangjiashan Barrier Lake. *Journal of Hydraulic Engineering* 136 (11): 914-923. [https://doi.org/10.1061/\(ASCE\)HY.1943-7900.0000241](https://doi.org/10.1061/(ASCE)HY.1943-7900.0000241)
- Lobovsky L, Botia E, Castellana F, et al. (2013) Experimental investigation of dynamic pressure loads during dam break. *Journal of Fluids and Structures* 48: 407-434. <https://doi.org/10.1016/j.jfluidstructs.2014.03.009>
- Mizuyama T, Tabata S, Mori T, et al. (2008) The dam break and prevention of barrier dam. *Water Resources and Hydropower Engineering* 39 (7): 97-99.
- Morris MW (2000) CADAM: Concerted Action on Dambreak Modelling. HR Wallingford Limited. Report No. 571, HR Wallingford Limited, Oxfordshire.
- Morris MW, Hassan M (2005) IMPACT: Investigation of extreme flood processes and uncertainty. No. EVG1-CT-2001-00037, Final technical report, Wallingford Ltd. <http://www.impact-project.net>
- Padulano R, Giudice GD (2016) Transitional and weir flow in a vented drop shaft with a sharp-edged intake. *Journal of Irrigation & Drainage Engineering* 142 (5): 6016002. [https://doi.org/10.1061/\(ASCE\)IR.1943-4774.0001011](https://doi.org/10.1061/(ASCE)IR.1943-4774.0001011)
- Peng M, Zhang L (2012) Breaching parameters of landslide dams. *Landslides* 9 (1): 13-31. <https://doi.org/10.1007/s10346-011-0271-y>
- Schuster RL, Costa JE (1986) A Perspective on Landslide Dams. Paper read at *Landslide Dams: Processes, Risk, and Mitigation*. Geotechnical Special Publication, No.3, ASCE, New York. pp 1-20
- Tacconi C, Segoni S, Casagli N, et al. (2016) Geomorphic indexing of landslide dams evolution. *Engineering Geology* 208: 1-10. <https://doi.org/10.1016/j.enggeo.2016.04.024>
- Wan C, Fell R (2004) Investigation of Rate of Erosion of Soils in Embankment Dams. *Journal of Geotechnical and Geoenvironmental Engineering* 130 (4): 373-380. [https://doi.org/10.1061/\(ASCE\)1090-0241\(2004\)130:4\(373\)](https://doi.org/10.1061/(ASCE)1090-0241(2004)130:4(373))
- Wang Q, Chen Z, Sui H, et al. (2011) Modelling seepage flow velocity in centrifuge models. *Chinese Journal of Geotechnical Engineering* (08): 1235-1239. (In Chinese)
- Wang W, Chen G, Zhang Y, et al. (2017) Dynamic simulation of landslide dam behavior considering kinematic characteristics using a coupled DDA-SPH method. *Engineering Analysis with Boundary Elements* 80: 172-183. <https://doi.org/10.1016/j.enganabound.2017.02.016>
- Wang X, Liang Z (2008) Experimental study on barrier dam break. *Technology of Soil and Water Conservation*: 8-9. (In Chinese) <https://doi.org/10.3969/j.issn.1673-5366.2008.02.004>
- Xuan K, Kim M, Nguyen H, et al. (2016) Analysis of Landslide Dam Failure Caused by Overtopping. *Procedia Engineering* 154: 990-994. <https://doi.org/10.1016/j.proeng.2016.07.587>
- Yan Z, Wei Y, Cai H (2009) Formation Mechanism and Stability Analysis of Barrier Dam. *The Chinese Journal of Geological Hazard and Control* 20 (04): 55-59. (In Chinese) <https://doi.org/10.3969/j.issn.1003-8035.2009.04.012>
- Yang F, Zhou X, Liu X, et al. (2011) Experimental study of breach growth processes in sand dams of quake lakes. *Journal of Earthquake and Tsunami* 05 (05): 445-459. <https://doi.org/10.1142/S179343111001182>
- Yang Y, Cao S, Yang K, et al. (2015) Experimental study of breach process of landslide dams by overtopping and its initiation mechanisms. *Journal of Hydrodynamics, Ser. B* 27(6): 872-883. [https://doi.org/10.1016/S1001-6058\(15\)60550-9](https://doi.org/10.1016/S1001-6058(15)60550-9)
- Zhao T, Chen S, Fu C, et al. (2017) Centrifugal model tests overtopping failure of barrier dams. *Chinese Journal of Geotechnical Engineering* 39 (10): 1943-1948. (In Chinese) <https://doi.org/10.11779/CJGE201611005>
- Zhong Q, Chen S, Deng Z (2018) Breach mechanism and numerical modeling of barrier dam due to overtopping failure. *SCIENTIA SINICA Technologica* 48: 959-968. (In Chinese) <https://doi.org/10.1360/No92017-00213>